AIP | Physics of Plasmas

Instability and dynamics of two nonlinearly coupled intense laser beams in a quantum plasma

Yunliang Wang, P. K. Shukla, and B. Eliasson

Citation: Phys. Plasmas **20**, 013103 (2013); doi: 10.1063/1.4774064
View online: http://dx.doi.org/10.1063/1.4774064
View Table of Contents: http://pop.aip.org/resource/1/PHPAEN/v20/i1
Published by the AIP Publishing LLC.

Instability and dynamics of two nonlinearly coupled intense laser beams in a quantum plasma

Yunliang Wang,[1,2] P. K. Shukla,[1,3,4] and B. Eliasson[1]
[1]*International Centre for Advanced Studies in Physical Sciences & Institute for Theoretical Physics, Faculty of Physics and Astronomy, Ruhr University Bochum, D-44780 Bochum, Germany*
[2]*Department of Physics, School of Mathematics and Physics, University of Science and Technology Beijing, Beijing 100083, China*
[3]*Department of Mechanical and Aerospace Engineering & Center for Energy Research, University of California San Diego, La Jolla, California 92093, USA*
[4]*School of Chemistry and Physics, KwaZulu-Natal University, Durban 4000, South Africa*

(Received 11 December 2012; accepted 17 December 2012; published online 8 January 2013)

We consider nonlinear interactions between two relativistically strong laser beams and a quantum plasma composed of degenerate electron fluids and immobile ions. The collective behavior of degenerate electrons is modeled by quantum hydrodynamic equations composed of the electron continuity, quantum electron momentum (QEM) equation, as well as the Poisson and Maxwell equations. The QEM equation accounts the quantum statistical electron pressure, the quantum electron recoil due to electron tunneling through the quantum Bohm potential, electron-exchange, and electron-correlation effects caused by electron spin, and relativistic ponderomotive forces (RPFs) of two circularly polarized electromagnetic (CPEM) beams. The dynamics of the latter are governed by nonlinear wave equations that include nonlinear currents arising from the relativistic electron mass increase in the CPEM wave fields, as well as from the beating of the electron quiver velocity and electron density variations reinforced by the RPFs of the two CPEM waves. Furthermore, nonlinear electron density variations associated with the driven (by the RPFs) quantum electron plasma oscillations obey a coupled nonlinear Schrödinger and Poisson equations. The nonlinearly coupled equations for our purposes are then used to obtain a general dispersion relation (GDR) for studying the parametric instabilities and the localization of CPEM wave packets in a quantum plasma. Numerical analyses of the GDR reveal that the growth rate of a fastest growing parametrically unstable mode is in agreement with the result that has been deduced from numerical simulations of the governing nonlinear equations. Explicit numerical results for two-dimensional (2D) localized CPEM wave packets at nanoscales are also presented. Possible applications of our investigation to intense laser-solid density compressed plasma experiments are highlighted. © *2013 American Institute of Physics*. [http://dx.doi.org/10.1063/1.4774064]

I. INTRODUCTION

The rapid development of laser technology, especially chirped pulse amplification (CPA), has provided excellent opportunities to construct table-top laser sources of femtosecond pulses with intensities up to 10^{22} W/cm^2,[1] and the next generation of powerful laser pulses that may reach intensities up to 10^{26} W/cm^2.[2] Such high power laser pulses will open a new window for carrying out research dealing with nonlinear interactions between intense laser beams and plasmas in the relativistic[3,4] and quantum regimes.[5] For hot plasmas (with the average plasma temperature T_p exceeding several tens of electron Volts) with extremely high plasma number densities (say, in the range $10^{23}-10^{28}$ cm^{-3}), the quantum mechanical effects ought to be considered, since the de Broglie thermal wave length λ_B of degenerate electrons and positrons could be comparable to the inter-electron/positron distance in a dense plasma;[6,7] typically, λ_B is much smaller than the Landau length e^2/k_BT_p, where e is the magnitude of the electron charge and k_B is the Boltzmann constant. Accordingly, there have been a number of recent investigations[5–7] that focused on nonlinear interactions between intense laser pulses and a dense quantum plasma that are relevant for the next-generation intense laser-solid density plasma experiments,[8] for quantum x-ray free-electron lasers (FELs),[9,10] for inertial confinement fusion (ICF) schemes,[11,12] and for localized x-ray pulses emanating from compact astrophysical objects.[13]

While investigating collective interactions in quantum plasmas, it is often convenient to use the quantum hydrodynamic (QHD) equations (or the Madelung equations for the quantum electron fluid) that is composed of the electron continuity, non-relativistic momentum equation for degenerate electron fluids, and Poisson's equation. The non-relativistic electron momentum equation (NREME) includes linear and nonlinear electron inertia, the electrostatic and Lorentz forces, as well as the quantum forces[14,15] arising from the quantum statistical pressure,[16] electron-exchange and electron correlation effects,[17] and the quantum recoil effect.[18] The latter reflects electron tunneling through the quantum Bohm potential and causes dispersion of electron wave functions at atomic scales. From the NREME, one can also derive a nonlinear Schrödinger equation (NLSEs) by invoking an eikonal representation that separates the amplitude and phases of electron wave functions. Quantum magnetohydrodynamic (QMHD)

equations[19] including electron spin-1/2 effect have been obtained from Pauli's equation, and used to investigate the spin-induced ponderomotive force.[20] Besides the above mentioned nonrelativistic hydrodynamic models, a relativistic quantum hydrodynamic equation has also been derived by using the Wigner distribution, where the quantum Bohm potential has been modified by the relativistic gamma factor.[21] In fact, the Dirac and Maxwell equations can be used to investigate the nonlinear propagation of intense laser pulses in quantum plasmas with electron spin effects.[22,23]

It is well known that nonlinear effects associated with the relativistic circularly polarized electromagnetic (CPEM) ponderomotive force and the relativistic electron mass increase in the CPEM wave fields produce stimulated scattering instabilities, two-plasmon decay instability,[24–28] as well as modulational and filamentational instabilities. In their classical Paper, Shukla and Eliasson[5] presented an investigation of nonlinear couplings between intense CPEM waves and quantum electron plasma oscillations (QEPOs) in a dense plasma. They accounted for relativistic electron mass increase in the CPEM fields and the RPF driven electron density variations and reported the parametric instabilities and trapping of a single CPEM wave into an electron hole at nanoscales in one-space dimension. Thus, two coupled nonlinear Schrödinger equations for the EM vector potential and the ES scalar potential were coupled with Poisson's equation to describe the behavior of nonlinearly coupled CPEM waves and QEPOs. It turns out that due to the quantum recoil effect in the dynamics of QEPOs, the electron number density remained non-zero in the RPF created density cavity, which is in sharp contrast to the classical plasma case,[29] where there could be a complete depletion of the electron number density.[29] Eliasson and Shukla[28] have investigated relativistic laser-plasma interactions in the quantum regime by using the Klein-Gordon equation to model the dynamics of relativistic electrons, where the main results of quasi-steady-state propagation are the same as that in Ref. 5. Furthermore, Eliasson and Shukla[9] also used the same mathematical model for relativistic X-ray free-electron lasers in the quantum regime, which can be used to explore matter at atomic and single molecule levels.[30] A two-stream instability and the quantum relativistic Buneman instabilities have also been investigated by using the Klein-Gordon-Maxwell system of equations.[31] Recently, stimulated Raman and Brillouin backscattering instabilities of coherent CPEM waves carrying orbital angular momentum have been investigated by considering quantum electron statistical pressure, electron-exchange, and electron-correlation effects, the quantum recoil effect in the dynamics of degenerate electrons that are participating in the driven QEPOs in a quantum plasma without and with strongly coupled ions.[15]

In this paper, we present an investigation of the parametric instabilities of two nonlinearly coupled intense laser beams in an unmagnetized quantum plasma. Nonlinear interactions between two laser beams in classical plasmas were investigated for realizing a plasma-based beat-wave accelerator scheme.[32] Here, large amplitude electron plasma waves can be nonlinearly excited by colliding two counter-propagating laser pulses.[33] Two counter-propagating intense laser pulses with tilted amplitude fronts can excite a standing plasma wave for accelerating electrons with energies reaching several GeV.[34] For two nonlinearly coupled laser beams in classic plasmas,[35] the dispersion relations for stimulated Raman and stimulated Brillouin scattering instabilities show rather weak interactions between the two-laser beams. New classes of the parametric instabilities were found in two-temperature electron plasmas.[36] Since the investigation of two nonlinearly coupled relativistically intense laser beams in quantum plasmas has important applications in the next-generation intense laser-solid density plasma interaction experiments, in X-ray free electron laser schemes, in laser-based inertial confinement fusion schemes, in high-energy charged particle acceleration schemes, as well as in astrophysical and cosmological environments, we shall use a useful model developed in Ref. 5 for studying the relativistic quantum modulational and stimulated scattering instabilities of two nonlinearly coupled CPEM waves and QEPOs and their nonlinear dynamics. In the dynamics of relativistic ponderomotive forces (RPF) driven QEPOs, we shall account for fully nonlinear quantum statistical pressure, the quantum electron recoil effect, as well as electron-exchange and electron correlation effects[37] and spin effects.[38] Thus, our previous investigation has been significantly enlarged to account for nonlinear interactions between intense two co-propagating intense laser beams and nonlinear QEPOs that will play a significant role in the nonlinear nanophysics of the next generation high density compressed plasmas produced by multiple intense laser beams for achieving ICF.

II. GOVERNING NONLINEAR EQUATIONS

Let us consider the nonlinear propagation of two nonlinearly coupled relativistically intense high-frequency CPEM pulses interacting with QEPOs in an unmagnetized quantum plasma with degenerate electron fluids and immobile ions. Accordingly, nonlinear phenomena would occur on time scales of the electron plasma period and uniformly distributed ions would not have time to respond to CPEM waves and QEPOs. Within the framework of a slowly varying envelope approximation, the two nonlinearly coupled intense CPEM waves can be described by two-coupled nonlinear Schrödinger equations[5]

$$2i\Omega_{01}\left(\frac{\partial}{\partial t}+\mathbf{v}_1\cdot\nabla\right)\mathbf{A}_1+\nabla^2\mathbf{A}_1-\left(\frac{|\psi|^2}{\gamma}-1\right)\mathbf{A}_1=0, \quad (1)$$

$$2i\Omega_{02}\left(\frac{\partial}{\partial t}+\mathbf{v}_2\cdot\nabla\right)\mathbf{A}_2+\nabla^2\mathbf{A}_1-\left(\frac{|\psi|^2}{\gamma}-1\right)\mathbf{A}_2=0, \quad (2)$$

where the vector potentials of the CPEM waves are $\mathbf{A}_j=A_j(\hat{\mathbf{x}}+i\hat{\mathbf{y}})\exp(-i\omega_{0j}t+i\mathbf{k}_{0j}\cdot\mathbf{r})$ with $j=1,\ 2$ and $\gamma=(1+|A_1|^2+|A_2|^2)^{1/2}$ is the relativistic gamma factor. Here, we have ignored the cross-coupling term $\mathbf{A}_1\cdot\mathbf{A}_2$, which has been considered in the context of the beat wave electron acceleration scheme,[32] and also in the ionospheric heating experiments.[36] Furthermore, $\Omega_{0j}=\omega_{0j}/\omega_{pe}(j=1,2)$ is the normalized CPEM waves frequency, and $\mathbf{v}_j=\mathbf{v}_{gj}/c$ is the normalized group velocity with $\mathbf{v}_{gj}=k_{0j}c^2/\omega_{0j}$, in which

ω_{0j} is the CPEM waves frequency, $\mathbf{k}_{0j}$ is the wave number, $\omega_{pe}=(4\pi n_0 e^2/m)^{1/2}$ is the electron plasma frequency, e is the magnitude of the electron charge, n_0 is the equilibrium electron number density, m is the electron rest mass, and c is the speed of light in vacuum. In the derivation of the coupled NLSEs, we used $\omega_{0j}^2=k_{0j}^2c^2+\omega_{pe}^2$. In Eqs. (1) and (2), the time and space variables are in units of the inverse plasma frequency ω_{pe}^{-1} and the electron inertial length $\lambda_e=c/\omega_{pe}$, respectively. The vector potential $\mathbf{A}_j$ is normalized by mc^2/e. The quantity $|\psi|^2$ is electron number density. The electron wave function ψ is also normalized by $n_0^{1/2}$, and given by

$$iH\frac{\partial\psi}{\partial t}+\frac{H^2}{2}\nabla^2\psi+(\phi-\gamma+1-\Gamma_F|\psi|^{4/D}-\Gamma_s\phi_{xc})\psi=0, \tag{3}$$

where the scalar potential ϕ is normalized by mc^2/e. The non-dimensional quantum parameter $H=\hbar\omega_{pe}/mc^2$ determines the relative importance of the quantum electron recoil effect. The second term in the left hand side of Eq. (3) is associated with the quantum Bohm potential. The relativistic ponderomotive potential $1-\gamma$ comes from the cross-coupling between electron quiver velocity and the magnetic field of the CPEM waves.[13,25] The term $\Gamma_F|\psi|^{4/D}\psi$ stands for the quantum statistic pressure coming from the Fermi electron pressure $P_e=m_eV_{Fe}^2n_0/3(n_e/n_0)^{D+2/D}$,[16,37,38] $V_F=(\hbar/m)(3\pi^2n_0)^{1/3}$ the Fermi speed, D is the number of space dimension of the system, the non-dimensional coefficient is $\Gamma_F=(V_F^2/c^2)(D+2)/6$, and $n_e=|\psi|^2$ is the electron number density. The last term $\Gamma_s\phi_{xc}\psi$ is electron-exchange and electron-correlation potentials due to electron spin, where the coefficient $\Gamma_s=0.985\,e^2/r_0mc^2$ and $r_0=n_0^{-1/3}$ is the Wigner-Seitz radius. Hence, the normalized potential is $\phi_{xc}=|\psi|^{2/3}+0.034a_B^{-1}ln(1+18.376a_B|\psi|^{2/3})$ and $a_B=\hbar^2/me^2r_0$ is the normalized Bohr radius by the Wigner-Seitz radius.[15,17,38,39] We stress that Eq. (3) for QEPOs includes the combined effects of the quantum electron wave function dispersion, the quantum statistical electron pressure, electron-exchange, and electron-correlation effects due to electron spin, and the relativistic ponderomotive forces of two intense laser pulses that are colliding in our quantum plasma. Equations (1)–(3) are closed by Poisson's equation

$$\nabla^2\phi=|\psi|^2-1. \tag{4}$$

Equations (1)–(4) reveal that nonlinear couplings between two intense CPEM waves and QEPOs emerged due to the nonlinear current density $|\psi|^2\mathbf{A}_j/\gamma$. The coupled Eqs. (1)–(4) can self-consistently describe two relativistically intense laser beams nonlinearly propagating in a quantum plasma, which can be used to investigate stimulated Raman scattering and modulational instabilities of two laser beams, as well as their nonlinear dynamics at nanoscales.

III. THE INSTABILITY AND DYNAMICS OF TWO LASER BEAMS

Here, we consider the parametric instabilities and the dynamics of two nonlinearly interacting intense CPEM waves in a quantum plasma. We first linearize our system of Eqs. (1)–(4) by introducing $\mathbf{A}_j(\mathbf{r},t)=[\mathbf{A}_{0j}+\mathbf{A}_{1j}(\mathbf{r},t)]\exp(-i\alpha_jt)(j=1,2)$, $\psi(\mathbf{r},t)=[1+\psi_1(\mathbf{r},t)]\exp(-i\beta t)$, and $\phi(\mathbf{r},t)=\phi_1(\mathbf{r},t)$, where $\mathbf{A}_{0j}$ are the large amplitude CPEM pump waves and $\mathbf{A}_{1j}$ are the small amplitude fluctuations of the CPEM waves. The frequency shifts can be determined by the equilibrium of Eqs. (1)–(4). The nonlinear frequency shift turns out to be $\alpha_j=(\gamma_0^{-1}-1)/2\Omega_{0j}(j=1,2)$, and $\beta=(\gamma_0-1)/H$ with $\gamma_0=(1+|A_{01}|^2+|A_{02}|^2)^{1/2}$. For first order quantities, we now introduce the Fourier representations as $\mathbf{A}_{1j}=\hat{\mathbf{A}}_{j+}\exp(i\mathbf{K}\cdot\mathbf{r}-i\Omega t)+\hat{\mathbf{A}}_{j-}\exp(-i\mathbf{K}\cdot\mathbf{r}+i\Omega t)(\mathrm{j}=1,2)$, $\psi_1=\hat{\psi}_+\exp(i\mathbf{K}\cdot\mathbf{r}-i\Omega t)+\hat{\psi}_-\exp(-i\mathbf{K}\cdot\mathbf{r}+i\Omega t)$, and $\phi_1=\hat{\phi}\exp(i\mathbf{K}\cdot\mathbf{r}-i\Omega t)+\hat{\phi}^*\exp(-i\mathbf{K}\cdot\mathbf{r}+i\Omega t)$, where Ω and K are the frequency and wave number of the QEPOs, respectively. Inserting these Fourier representations into the linearized equations (1)–(4), and then separating different Fourier modes and eliminating the Fourier coefficients, we obtain the nonlinear dispersion relation (NLDR)

$$\frac{1}{Q}+\left(\frac{1}{D_{1+}}+\frac{1}{D_{1-}}\right)|A_{01}|^2+\left(\frac{1}{D_{2+}}+\frac{1}{D_{2-}}\right)|A_{02}|^2=0, \tag{5}$$

where $D_{j\pm}=\mp2\Omega_{0j}(\Omega-\mathbf{K}\cdot\mathbf{v}_j)+K^2(j=1,2)$, the coupling constant is

$$Q=\frac{1}{2\gamma_0^3}\left(\frac{\gamma_0K^2}{D_L}-1\right), \tag{6}$$

and the QEPOs are represented by

$$D_L=\Omega^2-1-\frac{1}{4}H^2K^4-\frac{2}{3}\left(\frac{V_F^2}{c^2}+\frac{C_{xc}^2}{c^2}\right)K^2. \tag{7}$$

Here, the quantity $C_{xc}^2=0.985[1+0.62/(1+18.376\,a_B)]e^2/r_0m$. We note that the dispersion of the QEPOs $D_L=0$ is identical to that obtained by NLSE-Poisson system in a quantum plasma with degenerate electron fluids.[40] The quantum dispersion effects associated with the QEPO have recently been observed experimentally in a compressed plasma.[41]

Equation (5) covers both stimulated Raman scattering and modulational instabilities of two intense CPEM waves against QEPOs. If one of the amplitudes $|A_j|(j=1,2)$ is zero, then we can recover the nonlinear dispersion relation for a single laser beam propagating in a quantum plasma.[5]

In the following, we present results of the numerical analysis of Eq. (5) by assuming that the frequency has a complex value, of which the imaginary part represents the growth rate of instability. Without loss of generality, we choose $\mathbf{K}=K_y\hat{\mathbf{y}}+K_z\hat{\mathbf{z}}$ and $K^2=K_z^2+K_y^2$. We also use the dispersion relation $\omega_{0j}^2=k_{0j}^2c^2+\omega_{pe}^2$ that we used in the derivation of Eqs. (1) and (2). Instability essentially obeys the conservation of energy and momentum $\Omega_j=\Omega_s+\Omega$ and $\mathbf{k}_j=\mathbf{k}_s+\mathbf{K}$, where Ω_j and $\mathbf{k}_j$ are the frequency and wave numbers of the pump waves, Ω_s and $\mathbf{k}_s$ are the frequency and wave numbers for the scattered and frequency downshifted electromagnetic daughter wave, Ω and $\mathbf{K}$ are the frequency and wave numbers of the QEPOs. We thus have the matching condition $(1+k_j^2)^{1/2}=[1+(\mathbf{k}_j-\mathbf{K})^2]^{1/2}+[1+H^2K^4/4+(2/3)(V_F^2+C_{xc}^2)K^2/c^2]^{1/2}$, which relates the components K_y and K_z of the QEPOs to each other and gives rise to approximately circular regions, which can be seen in Fig. 1.

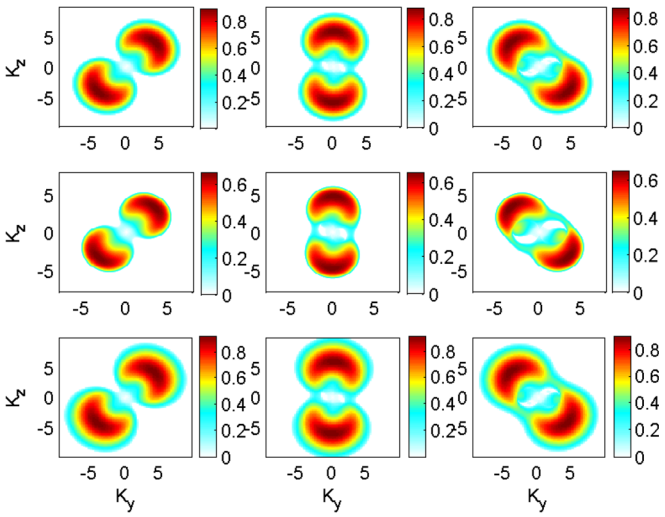

FIG. 1. The growth rate of stimulated Raman scattering instability as a function of the wave numbers K_y and K_z. The parameters are $H=0.001$, $V_F/c=0.069$, $C_{xc}/c=0.013$ for upper row and $H=0.007$, $V_F/c=0.257$, $C_{xc}/c=0.025$ for middle row of panels. The parameters for the lower row are $H=0.007$, $V_F/c=0$, $C_{xc}/c=0$. The directions of the two laser beams propagation are $(\theta_1,\theta_2)=(\pi/4,\pi/4)$, $(\pi/4,\pi/2)$, and $(\pi/4,3\pi/4)$ for the left, middle, and right column of the panels, respectively.

Now let us evaluate the quantum parameters $H=\hbar\omega_{pe}/mc^2$, V_F/c, and C_{xc}/c by using the typical dense plasma system. For intense laser solid density plasma interaction experiments, and for the next generation of laser-based plasma compression (LBPC) experiment, the electron number density n_0 can reach $10^{23}\text{cm}^{-3}\sim10^{28}\text{cm}^{-3}$.[5,13,42] Henceforth, the quantum parameters H may be in the range $2.29\times10^{-5}\sim0.007$, while V_F/c is in the range $0.005\sim0.25$ and C_{xc}/c is in the range $0.004\sim0.02$.

We have solved the nonlinear dispersion relation (5) and presented the numerical results in Figs. 1 and 2. The nonlinear couplings between two laser beams with QEPOs give

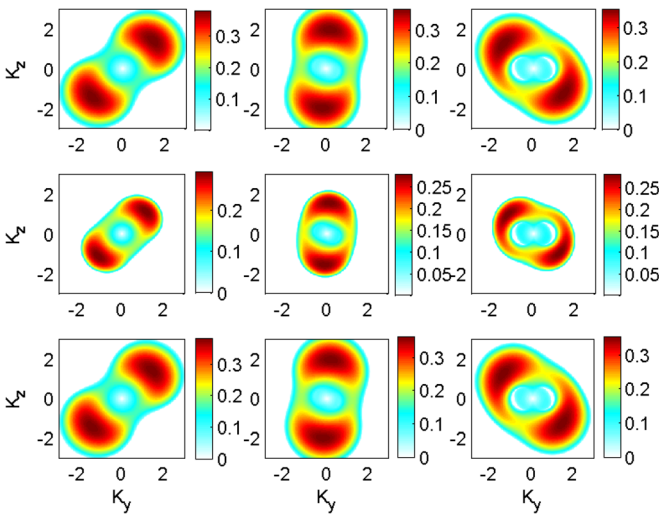

FIG. 2. The growth rate of the modulational instability as a function of the wave numbers K_y and K_z. The parameters are $H=2.3\times10^{-5}$ with $V_F/c=0.005$ and $C_{xc}/c=0.003$, $H=0.007$ with $V_F/c=0.257$ and $C_{xc}/c=0.025$, $H=0.007$ with $V_F/c=0$ and $C_{xc}/c=0$ for upper row, middle row, and lower row of panels, respectively. The directions of the two laser beams propagation are the same as those in Fig. 1.

Raman scattering instability, of which the growth rate is given in Fig. 1. We assume that the two laser beams propagate in the y and z directions and have the wave numbers $(k_{jy},k_{jz})=(1-1/\Omega_{0j}^2)^{1/2}(\cos\theta_j,\sin\theta_j)(j=1,2)$ with $(\theta_1,\theta_2)=(\pi/4,\pi/4)$, $(\pi/4,\pi/2)$, and $(\pi/4,3\pi/4)$ for the left, middle, and right column of the panels, respectively. For all cases in Fig. 1, we used $|A_{01}|=1,|A_{02}|=2$ and $\Omega_{01}=2$, $\Omega_{02}=3$. One can use the dispersion relation $\omega_{0j}^2=k_{0j}^2c^2+\omega_{pe}^2$ to determine the wave numbers of the two laser beams. In order to illustrate the effects of the quantum dispersion, the quantum statistical pressure, electro- exchange, and electron-correlation potentials on the Raman scattering growth rate, we used the parameters, $H=0.001$, $V_F/c=0.069$, and $C_{xc}/c=0.013$ in the upper row of the panels and considered the quantum dispersion effect with $H=0.007$ both in the middle and lower rows of the panels. But we took $V_F/c=0.257$, $C_{xc}/c=0.025$ for middle row and $V_F/c=0$, $C_{xc}/c=0$ for lower row of the panels in Fig. 1. We observe that the dispersion relation shows a rather strong interaction between the two laser beams and the growth rate is larger for $H=0.001$ than that for $H=0.007$. The propagation of the scattered wave is almost identical to the laser beam with the vector potential A_2. For stronger quantum effects, we observe a new class of the parametric instability that is, however, weaker than that of a weaker quantum effect. From the left, middle, and right column of the panels in Fig. 1, one can confirm that the interaction between two laser beams is strongest and the corresponding growth rate is the largest when the two laser beams propagate along the same direction. To consider the effects of the quantum statistic pressure and electron-exchange, and electron-correlation potential on the growth rate, we let $V_F/c=0$, $C_{xc}/c=0$ in the lowest row, which shows that the presence of the quantum statistical and electron-exchange and electron-correlation potential will decrease the growth rate moderately. In fact, in Fig. 2, we see that the quantum statistical effect and electron-exchange and electron-correlation potential effects will have great influence on the modulational instability that dominates as the pump frequencies are smaller than twice the plasma frequencies, which can be illustrated by the dispersion relations of the QEPOs, $D_L=0$. The dispersion relation gives two distinct dispersion effects. One is the long wavelength regime with $H^2K^2\ll(8/3)(V_F^2/c^2+C_{xc}^2/c^2)$ and the other is the short wavelength regime with $H^2K^2\gg(8/3)(V_F^2/c^2+C_{xc}^2/c^2)$.[7] Then two regimes are separated by the normalized critical wave number

$$K_c=\left(\frac{2}{3}\right)^{\frac{1}{2}}\frac{1}{Hc}(V_F^2+C_{xc}^2)^{\frac{1}{2}}\sim\frac{c}{\omega_{pe}}n_0^{\frac{1}{3}}. \tag{8}$$

The modulational instability occurs for small wave numbers and the quantum statistics effect will dominates in the long wavelength regime. In Fig. 2, we used $|A_{01}|=1,|A_{02}|=2$ and $\Omega_{01}=\Omega_{02}=1.2$ for all cases. For investigating the quantum effects on the modulational instability growth rate, we used the parameters $H=2.3\times10^{-5}$, $V_F/c=0.005$, and $C_{xc}/c=0.003$ as $n_0=10^{23}\text{cm}^{-3}$ in the upper row of panels and considered the parameters $H=0.007$ with $n_0=10^{28}\text{cm}^{-3}$ both in middle and in lower rows of the panels in Fig. 2. In

the middle row of the panels, the quantum statistical parameter is $V_F/c = 0.257$ and the electron-exchange and electron-correlation potentials which yield $C_{xc}/c = 0.025$, and in the lower row of panels the quantum statistical and electron-exchange and electron-correlation potentials are absent. We also assume the two laser beams propagate in the y and z directions and have the wave numbers $(k_{jy}, k_{jz}) = (1 - 1/\Omega_{0j}^2)^{1/2}(\cos\theta_j, \sin\theta_j)(j = 1, 2)$ with the same angle (θ_1, θ_2) as those in Fig. 1 for left, middle, and right column of panels, respectively. One can conclude that the modulational instability growth rate will decrease with the quantum effect increasing when one consider quantum statistical pressure. However, the growth rate will increase with the quantum effect when the quantum statistical effect is absent. The fastest growing waves propagate almost along the laser beam two.

In order to investigate the nonlinear dynamics of the two-laser beams interaction in our quantum plasma, we have carried out numerical simulations of the reduced system of Eqs. (1)–(4) in two-space dimension. In Fig. 3, we display the numerical results for stimulated Raman scattering, where we have used as an initial condition that the amplitudes of the two laser beams are $|A_{01}| = 1, |A_{02}| = 2$, and the corresponding frequency are $\Omega_{01} = 2, \Omega_{02} = 3$, respectively. As one can see, the scattering instability illustrated in Fig. 1, the corresponding growth rate is the largest when the two laser beams propagate along the same direction. The background plasma density is slightly perturbed with a low-level noise (random numbers). We consider the two pump laser beams propagating along the same direction. Our results show that the growing waves propagate along the same direction as the pump laser beam two with larger frequency and larger amplitude, which agree with the fastest growing wave in Fig. 1. During the initial exponential growth phase at $t = 20$, the two laser beams are strongly coupled with each other. The potential ϕ also reach maxima when the two laser beams simultaneously reach

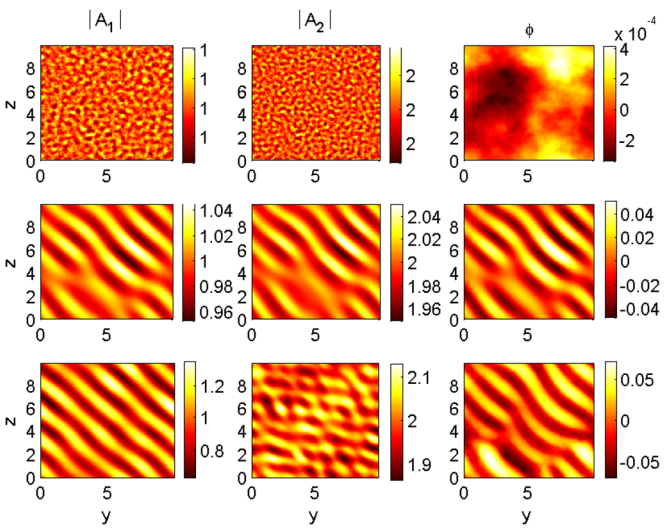

FIG. 3. The dynamics involving stimulated Raman scattering instability of the two laser beams propagating in the same directions as $(\theta_1, \theta_2) = (\pi/4, \pi/4)$ at times $t = 0.1$, $t = 20$, $t = 50$ (upper to lower panels). The other parameters are $H = 0.001$ and $V_F/c = 0.069$, $C_{xc}/c = 0.013$. The upper, middle, and lower rows of the panels are in corresponding to the amplitudes of the laser beam $|A_1|$, $|A_2|$, and the scalar potential ϕ, respectively.

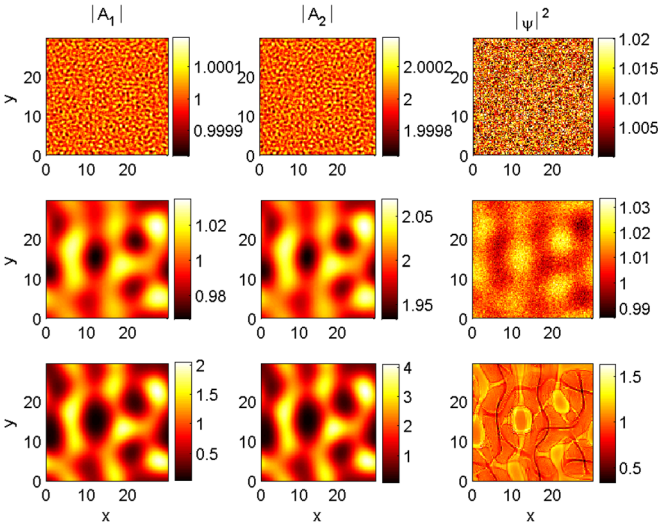

FIG. 4. The dynamics involving modulational instability of the two laser beams in the (x, y) plane perpendicular to the directions of the propagation of the two laser beams at times $t = 0.1$, $t = 40$, $t = 60$ (upper to lower panels). The other parameters are $H = 0.002$ with $V_F/c = 0.119$ and $C_{xc}/c = 0.016$. The upper, middle, and lower rows of the panels are in corresponding to the amplitudes of the laser beam $|A_1|$, $|A_2|$, and the electron number density $|\psi|^2$, respectively.

maxima. At time $t = 50$, the two laser beams do not have same locations in space, as nonlinear saturation occurs. In Fig. 4, we present the modulational instability dynamics by considering the frequency of the pump waves smaller than twice the plasma frequency. The pump waves are propagating in the z direction in an initially homogeneous plasma with a low-level noise. We only consider the instability giving rise to perturbations in the (x, y) plane. Our numerical results show that the self-focusing and collapse of wave packets occur at different times. In the lower row of panels in Fig. 4, the CPEM wave packets are trapped in a quantum electron hole when the nonlinear saturation of the modulational instability occur. Here, we used $|A_{01}| = 1, |A_{02}| = 2$, and $\Omega_{01} = \Omega_{02} = 1.2$. The results show that the quantum dispersion effects can greatly influence the Raman instability and have small impact on the modulational instability, which was due to the fact that modulational instability takes place at small wave number.[28] Furthermore, the quantum statistical effect and electron-exchange and electron-correlation potentials have great influence on the modulational instability of the two laser beams.

IV. SUMMARY AND CONCLUSIONS

In this paper, we have investigated parametric instabilities and the dynamics of two nonlinearly coupled intense laser beams in a quantum plasma. For our purposes, we have obtained three coupled nonlinear Schrödinger equations and Poisson's equation for CPEM waves that are interacting with nonlinear QEPOs. The coupling between the CPEM wave fields and nonlinear QEPOs comes through the nonlinear current $|\psi|^2\mathbf{A}_j/\gamma$ in the Maxwell equations. The dynamical equations for the driven (by relativistic ponderomotive forces of two intense CPEM waves) QEPOs include the new physics of the quantum statistical electron pressure, the quantum electron recoil effect, as well as electron-exchange

and electron-correlation effects caused by degenerate electron spin. We have carried out the Fourier analysis of our nonlinearly coupled wave equations to obtain the general nonlinear dispersion relation that predict stimulated Raman scattering and modulational instabilities of two co-propagating intense CPEM waves in a quantum plasma. We numerically analyzed the growth rate and the fastest growing mode of stimulated Raman scattering instability and found maximum values when the two pump CPEM waves propagate along the same direction. Both quantum dispersion and quantum statistical pressure effects lead to a decrease of the Raman instability growth rate. The quantum statistical pressure has larger influence on the modulational instability than on stimulated Raman instability, which is due to the fact that the quantum statistical pressure will dominate in the long wavelength regime as the modulational instability occurs at small wave numbers. The numerical results of the dynamics of two laser beams for the pump frequency $\Omega_{0j} < 2$ confirm that when the nonlinear saturation of the modulational instability occurs, localized CPEM wave packets are trapped in a quantum electron hole that is supported by the quantum forces of degenerate electrons and relativistic ponderomotive forces of two intense CPEM waves in a quantum plasma at nanoscales. The results of our investigation should be useful in understanding nonlinear instability and the dynamics of two nonlinearly coupled intense CPEM waves in the next-generation of compressed plasmas which surpass solid densities.

ACKNOWLEDGMENTS

One of the authors (Y.W.) thanks the support of NSFC (No. 11104012) and the Fundamental Research Funds for the Central Universities (No. FRF-TP-09-019A).

[1]V. Yanovsky, V. Chvykov, G. Kalinchenko, P. Rousseau, T. Planchon, T. Matsuoka, A. Maksimchuk, J. Nees, G. Cheriaux, G. Mourou, and K. Krushelnick, Opt. Express **16**, 2109 (2008).
[2]M. Dunne, Nature Phys. **2**, 2 (2006).
[3]G. A. Mourou, T. Tajima, and S. V. Bulanov, Rev. Mod. Phys. **78**, 309 (2006).
[4]M. Marklund and P. Shukla, Rev. Mod. Phys. **78**, 591 (2006).
[5]P. K. Shukla and B. Eliasson, Phys. Rev. Lett. **99**, 096401 (2007).
[6]P. K. Shukla and B. Eliasson, Phys. Usp. **53**, 51 (2010).
[7]P. K. Shukla and B. Eliasson, Rev. Mod. Phys. **83**, 885 (2011).
[8]S. M. Vinko, O. Ciricosta, B. I. Cho, K. Engelhorn, H.-K. Chung, C. R. D. Brown, T. Burian, J. Chalupský, R. W. Falcone, C. Graves, V. Hájková, A. Higginbotham, L. Juha, J. Krzywinski, H. J. Lee, M. Messerschmidt, C. D. Murphy, Y. Ping, A. Scherz, W. Schlotter, S. Toleikis, J. J. Turner, L. Vysin, T. Wang, B. Wu, U. Zastrau, D. Zhu, R. W. Lee, P. A. Heimann, B. Nagler, and J. S. Wark, Nature (London) **482**, 59 (2012).
[9]B. Eliasson and P. K. Shukla, Phys. Rev. E **85**, 065401 (2012).
[10]A. Serbeto, L. F. Monteiro, K. H. Tsui, and J. T. Mendonça, Plasma Phys. Controlled Fusion **51**, 124024 (2009).
[11]H. Azechi and the FIREX Project, Plasma Phys. Controlled Fusion **48**, B267 (2006).
[12]H. Hora, R. Sadighi-Bonabi, and E. Yazdani, Phys. Rev. E **85**, 036404 (2012).
[13]A. K. Harding and D. Lai, Rep. Prog. Phys. **69**, 2631 (2006).
[14]F. Haas, Phys. Plasmas **12**, 062117 (2005).
[15]P. K. Shukla, B. Eliasson, and L. Stenflo, Phys. Rev. E **86**, 016403 (2012).
[16]G. Manfredi and F. Hass, Phys. Rev. B **64**, 075316 (2001).
[17]L. Brey, J. Dempsey, N. F. Johnson, and B. I. Halperin, Phys. Rev. B **42**, 1240 (1990).
[18]H. E. Wilhelm, Z. Phys. **241**, 1 (1971).
[19]M. Marklund and G. Brodin, Phys. Rev. Lett. **98**, 025001 (2007).
[20]G. Brodin, A. P. Misra, and M. Marklund, Phys. Rev. Lett. **105**, 105004 (2010).
[21]J. Zhu and P. Ji, Phys. Rev. E **81**, 036406 (2010).
[22]J. T. Mendonça and A. Serbeto, Phys. Rev. E **83**, 026406 (2011).
[23]B. Eliasson and P. K. Shukla, Phys. Rev. E **84**, 036401 (2011).
[24]S. Guérin, G. Laval, P. Mora, J. C. Adam, A. Héron, and A. Bendib, Phys. Plasmas **2**, 2807 (1995).
[25]C. J. McKinstrie and R. Bingham, Phys. Fluids B **4**, 2626 (1992).
[26]L. Stenflo, B. Eliasson, and M. Marklund, J. Plasma Phys. **74**, 371 (2008).
[27]J. F. Drake, P. K. Kaw, Y. C. Lee, G. Schmidt, C. S. Liu, and M. N. Rosenbluth, Phys. Fluids **17**, 778 (1974).
[28]B. Eliasson and P. K. Shukla, Phys. Rev. E **83**, 046407 (2011).
[29]D. Farina and S. V. Bulanov, Phys. Rev. Lett. **86**, 5289 (2001).
[30]L. Young, E. P. Kanter, B. Krössig, Y. Li, A. M. March, S. T. Pratt, R. Santra, S. H. Southworth, N. Rohringer, L. F. DiMauro, G. Doumy, C. A. Roedig, N. Berrah, L. Fang, M. Hoener, P. H. Bucksbaum, J. P. Cryan, S. Ghimire, J. M. Glownia, D. A. Reis, J. D. Bozek, C. Bostedt, and M. Messerschmidt, Nature (London) **466**, 56 (2010).
[31]F. Haas, B. Eliasson, and P. K. Shukla, Phys. Rev. E **85**, 056411 (2012); F. Haas, B. Eliasson, and P. K. Shukla, *ibid.* **86**, 036406 (2012).
[32]R. Bingham, J. T. Mendonça, and P. K. Shukla, Plasma Phys. Controlled Fusion **46**, R1 (2004).
[33]Z.-M. Sheng, K. Mima, Y. Sentoku, K. Nishihara, and J. Zhang, Phys. Plasmas **9**, 3147 (2002).
[34]A. L. Galkin, V. V. Korobkin, M. Yu. Romanovskiy, V. A. Trofimov, and O. B. Shiryaev, Phys. Plasmas **19**, 073102 (2012).
[35]P. K. Shukla, B. Eliasson, M. Marklund, L. Stenflo, I. Kourakis, M. Parviainen, and M. E. Dieckmann, Phys. Plasmas **13**, 053104 (2006).
[36]B. Eliasson and P. K. Shukla, Phys. Rev. E **74**, 046401 (2006).
[37]P. K. Shukla and B. Eliasson, Phys. Rev. Lett. **96**, 245001 (2006).
[38]N. Crouseilles, P.-A. Hervieux, and G. Manfeidi, Phys. Rev. B **78**, 155412 (2008).
[39]P. K. Shukla and B. Eliasson, Phys. Rev. Lett. **108**, 165007 (2012).
[40]D. Pines, Phys. Rev. **92**, 626 (1953); D. Bohm and D. Pines, *ibid.* **92**, 609 (1953).
[41]S. H. Glenzer, O. L. Landen, and P. Neumayer, Phys. Rev. Lett. **98**, 065002 (2007).
[42]J. Zhu and P. Ji, Plasma Phys. Controlled Fusion **54**, 065004 (2012).